Supporting Information

The synthesis and mechanistic studies of a highly active nickel phosphide catalyst for naphthalene hydrodearomatization

Guoxia Yun,[a] Qingxin Guan,[*a] Wei Li[*ab]

a. College of chemistry, Key laboratory of advanced energy materials chemistry (Ministry of Education), Nankai University, Tianjin, 300071, China.
b. Collaborative Innovation Center of Chemical Science and Engineering, Tianjin, 300071, China.
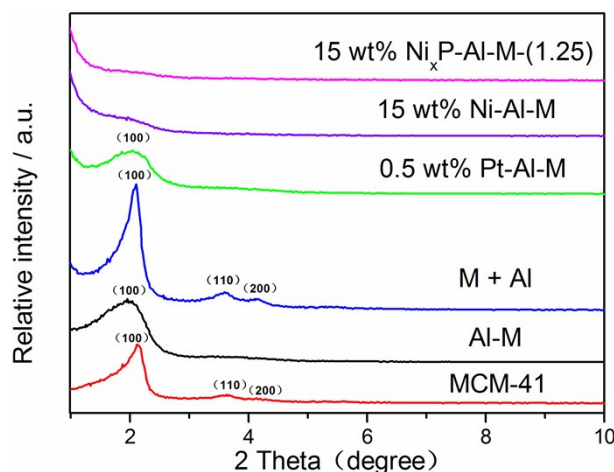*Corresponding author: weili@nankai.edu.cn, qingxinguan@nankai.edu.cn

Fig. S1 Low-angle powder X-ray diffraction patterns of MCM-41, Al-M, physical mixture (M+Al) supports and the Pt-, Ni-, Ni_xP-based catalysts.
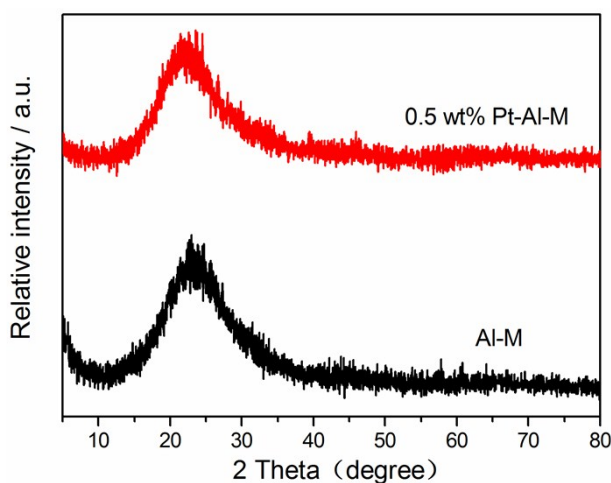

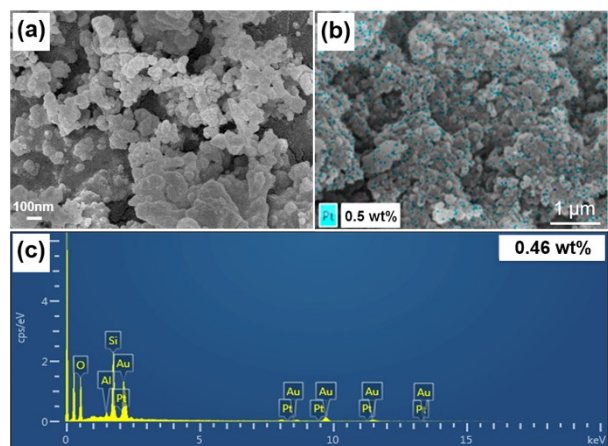**Fig. S2** XRD patterns of Al-M support along with the corresponding Pt-loaded catalyst.

Fig. S3 The SEM (a), mapping image (cyan dot refer to platinum atom) (b), and EDS (c) of 0.5 wt% Pt-Al-M catalyst.
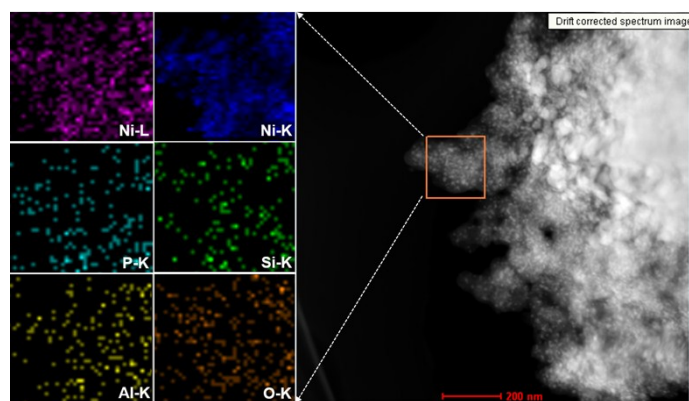

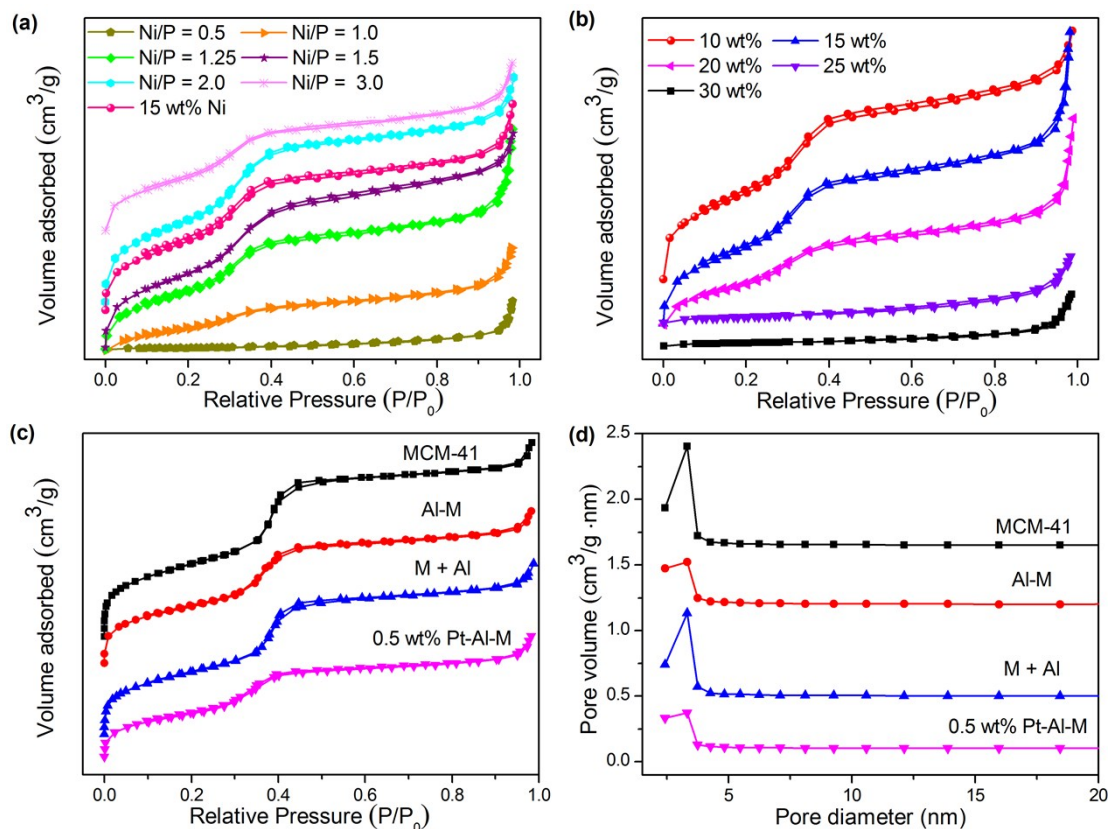**Fig. S4** HAADF-STEM micrographs of 15 wt% Ni_xP-Al-M-(1.25).

Fig. S5 The N$_2$ adsorption-desorption isotherms of (a) 15 wt% Ni$_x$P-Al-M with various initial Ni/P molar ratios, (b) Ni$_x$P-Al-M-(1.25) with different Ni$_x$P loadings, (c) MCM-41, Al-M, physical mixture (M+Al) supports, 0.5 wt% Pt-Al-M catalyst and (d) the corresponding BJH pore size distributions of supports and 0.5 wt% Pt-Al-M catalyst.
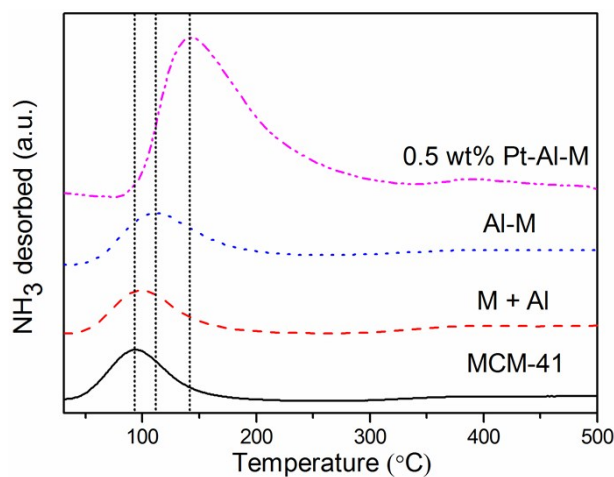

Fig. S6 Temperature programmed desorption of ammonia (NH$_3$-TPD) profiles for supports MCM-41, physical mixture (M+Al), Al-M supports, and 0.5 wt% Pt-Al-M catalyst.

Table S1

Textural and structural properties of the different supports and prepared catalysts obtained from N_2 physisorption measurements.

	Samples	S_{BET}^a $(m^2 g^{-1})$	V_{BJH}^b $(cm^3 g^{-1})$	D_{mp}^c (nm)	Average crystallite size^d (nm)
	MCM-41	893	0.96	3.3	-
Support	Al-M	720	0.79	3.3	-
	M+Al	777	0.85	3.3	-
	0.5 wt% Pt-Al-M-(1.25)	595	0.61	2.4	-
	15 wt% Ni_xP-MCM-41-(1.25)	471	0.40	2.4	16.85
Catalysts with	15 wt% Ni-Al-M-(1.25)	420	0.42	2.4	13.68
different	10 wt% Ni_xP-Al-M-(1.25)	387	0.38	2.4	-
loadings	15 wt% Ni_xP-Al-M-(1.25)	357	0.44	2.4	15.35
	20 wt% Ni_xP-Al-M-(1.25)	234	0.32	2.4	23.43
	25 wt% Ni_xP-Al-M-(1.25)	213	0.18	2.4	17.46
	30 wt% Ni_xP-Al-M-(1.25)	170	0.18	2.4	26.62
Catalysts with	15 wt% Ni_xP-Al-M-(0.5)	170	0.18	2.4	23.69
different	15 wt% Ni_xP-Al-M-(1.0)	184	0.22	2.4	18.27
initial Ni/P	15 wt% Ni_xP-Al-M-(1.25)	357	0.44	2.4	15.35
molar ratios	15 wt% Ni_xP-Al-M-(1.5)	433	0.43	2.4	19.16
	15 wt% Ni_xP-Al-M-(2.0)	473	0.45	2.4	20.28
	15 wt% Ni_xP-Al-M-(3.0)	492	0.47	2.4	20.32

a   BET surface area calculated from the adsorption branch of the N_2 isotherm.

b   Total pore volumes calculated from the N_2 adsorption at relative pressure (P/P$_0$) of 0.98.

c   Mesopore diameter calculated from the adsorption branch of the N_2 isotherm using the BJH method.

d   The crystallite size calculated from Scherrer's equation according to the full width at half maximum (FWHM) applied to the most intense diffraction peak.

-: The species was not detected.

Table S2

Observed metal content and Ni/P molar ratio of catalysts compared to theoretical Ni/P using ICP-OES.

Samples	Metal content（wt.%）		Theoretical Ni/P molar ratio	Observed Ni/P molar ratio
	Al	Ni		
Al-M	4.7	-	-	-
15 % Ni_xP-Al-M-(0.5)	4.7	8.95	0.5	0.84
15 % Ni_xP-Al-M-(1.0)	4.7	10.3	1.0	1.81
15 % Ni_xP-Al-M-(1.25)	4.7	10.0	1.25	2.14
15 % Ni_xP-Al-M-(1.5)	4.7	10.7	1.5	2.60
15 % Ni_xP-Al-M-(2.0)	4.7	11.3	2.0	3.54
15 % Ni_xP-Al-M-(3.0)	4.7	11.0	3.0	5.12

-:The species was not detected.

Table S3

XPS analysis results along with (Ni/P) nominal atomic ratio.

Samples	superficial atomic ratio(Ni/P)	Ni (wt %)	P (wt %)	Binding energy (eV)		Binding energy (eV)	
				Ni $2p_{3/2}$		P 2p	
				Ni^{2+}	$Ni^{\delta+}$	PO_4^{3-}	$P^{\delta-}$
15 wt% Ni_xP-MCM-41-(1.25)	0.48	1.2	2.5	856.4	852.3	134.5	129.5
15 wt% Ni_xP-Al-M-(1.25)	0.53	0.8	1.5	856.4	852.3	134.5	129.5

Table S4

The corresponding NH_3-TPD characterization, CO chemisorption uptakes, and turnover frequency (TOF) of the samples.

Samples	NH_3-TPD[a]			CO uptakes ($\mu mol\ g^{-1}$)	TOF (s^{-1})
	Peak temperature (°C)	Area percentage in parenthesis	Total acidity normalized to the acidity of pure Al-M		
MCM-41	94	(100%)	0.66	-	-
Al+M	98	(100%)	0.62	-	-
Al-M	115	(100%)	1.00	-	-
15 wt% Ni_xP-MCM-41-(1.25)	116	(100%)	0.28	2.8	0.42
15 wt% Ni-Al-M-(1.25)	112; 425	(65%); (45%)	0.81; 0.56	3.1	0.44
15 wt% Ni_xP-Al-M-(0.5)	-	-	-	2.8	0.43
15 wt% Ni_xP-Al-	117	(100%)	1.48	3.0	0.43

M-(1.0)					
15 wt% Ni$_x$P-Al-M-(1.25)	112	(100%)	1.47	3.1	0.44
15 wt% Ni$_x$P-Al-M-(1.5)	105	(100%)	1.19	3.0	0.44
15 wt% Ni$_x$P-Al-M-(2.0)	99	(100%)	1.06	2.9	0.43
15 wt% Ni$_x$P-Al-M-(3.0)	108	(100%)	0.64	2.8	0.43

[a] As determined by the TPD-NH$_3$ analysis and normalized to the acidity of pure Al-M.
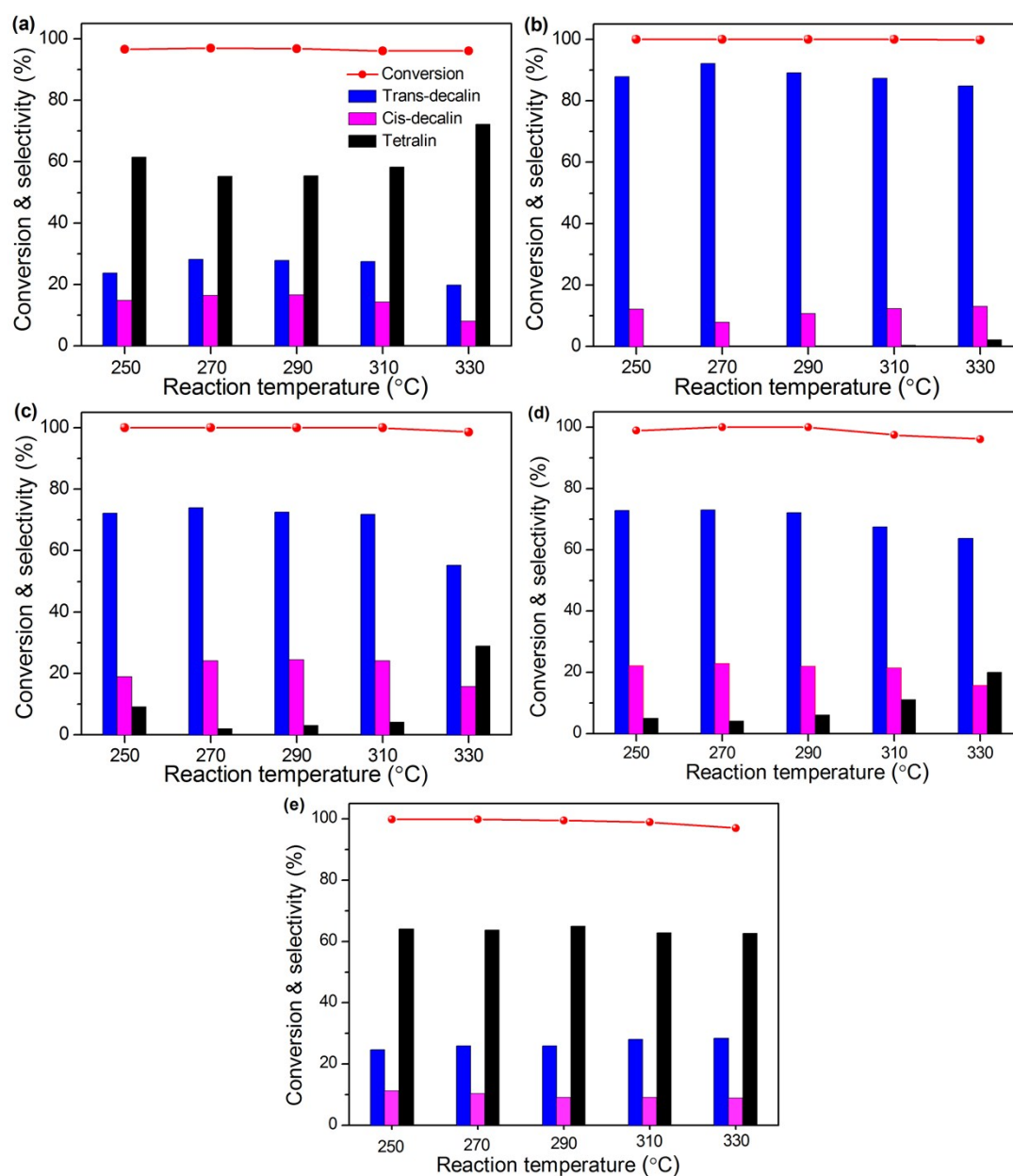
-:The species was not detected.

Fig. S7 Product distribution of naphthalene HYD over Ni$_x$P-Al-M-(1.25) with different Ni$_x$P loadings as a function of temperature, (a) 10 wt%, (b) 15 wt%, (c) 20 wt%, (d) 25 wt%, and (e) 30 wt%.
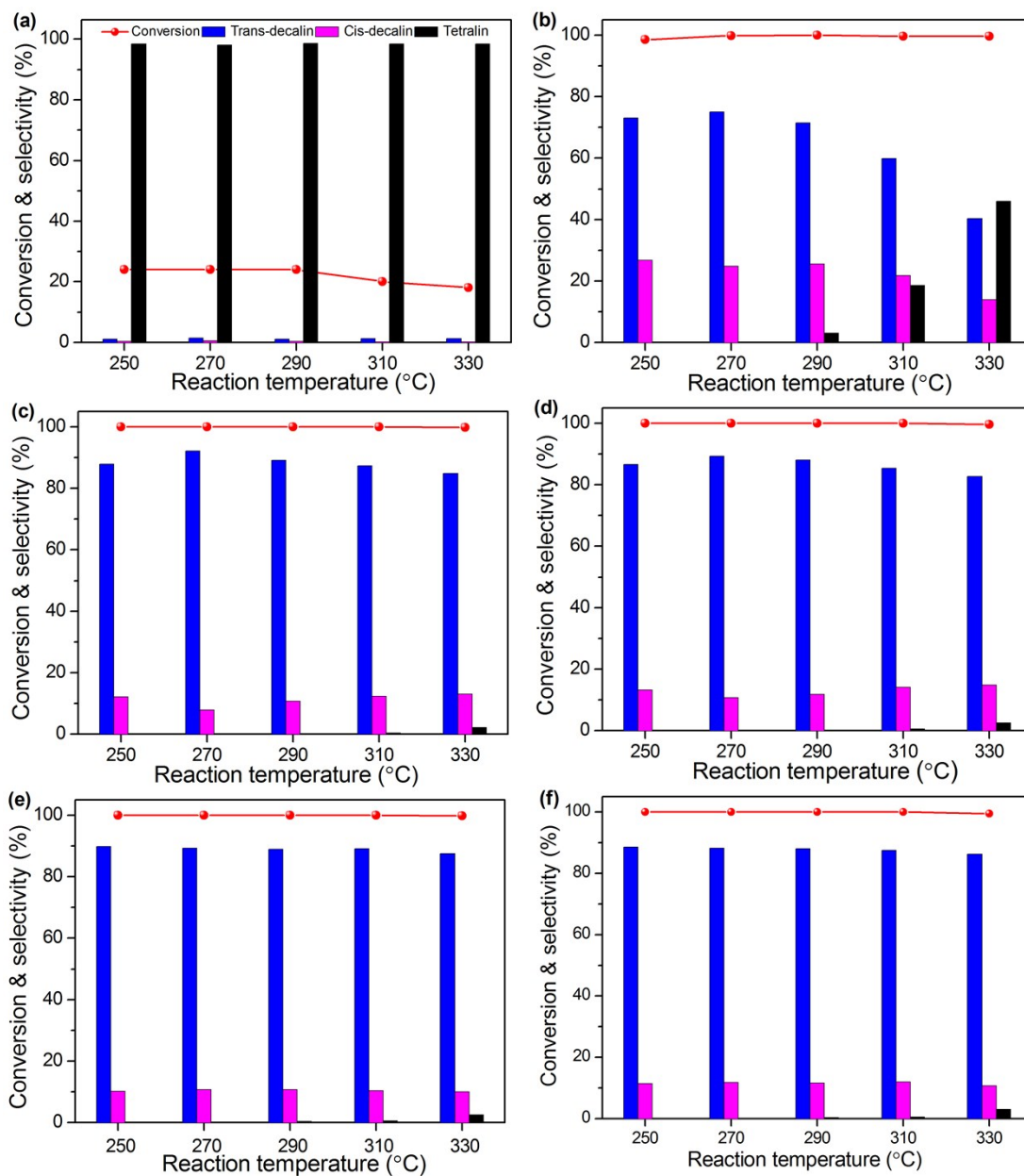
Fig. S8 Product distribution of naphthalene HYD over 15 wt% Ni$_x$P-Al-M with the precursor of different Ni/P molar ratio as a function of temperature. (a) 0.5, (b) 1.0, (c) 1.25, (d) 2.0, (e) 2.0, and (f) 3.0.
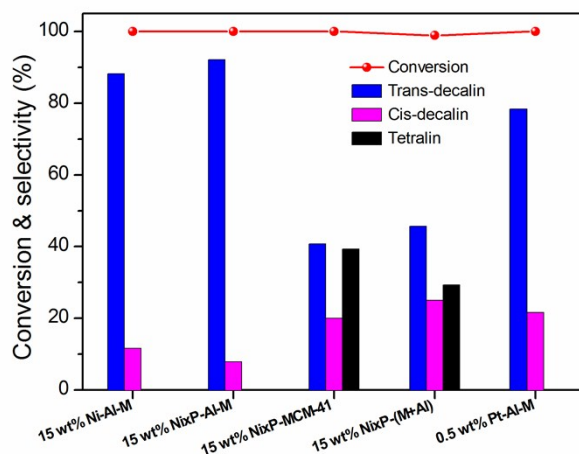
Fig. S9 Naphthalene conversion and product selectivities with reaction temperature of 270 °C over Ni, Ni$_x$P, and Pt supported catalysts.
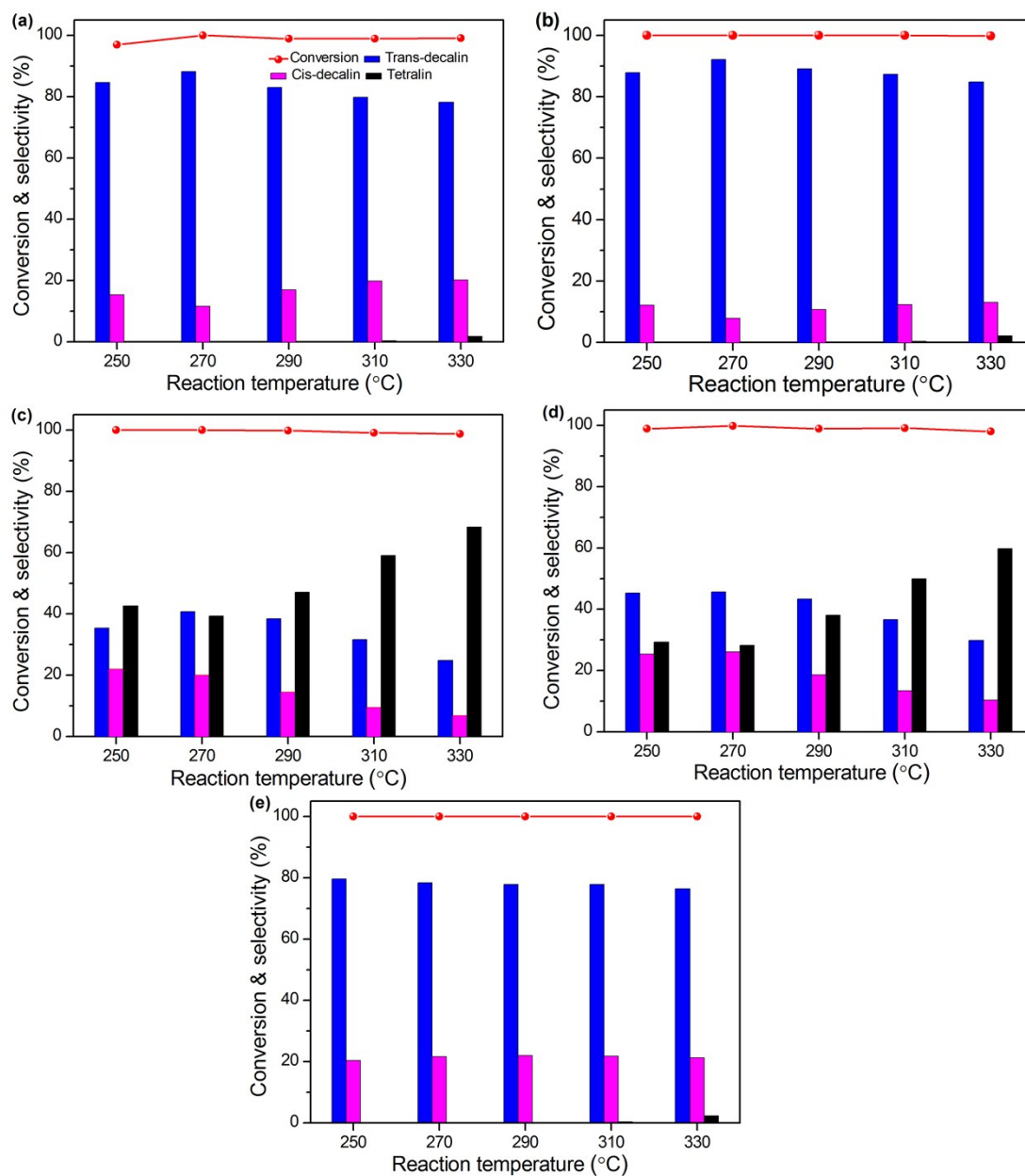

Fig. S10 Product distribution of naphthalene HYD over different catalysts as a function of temperature. (a) 15 wt% Ni-Al-M, (b) 15 wt% Ni$_x$P-Al-M, (c) 15 wt% Ni$_x$P-MCM-41, (d) 15 wt% Ni$_x$P-(M+Al), and (e) 0.5 wt% Pt-Al-M.
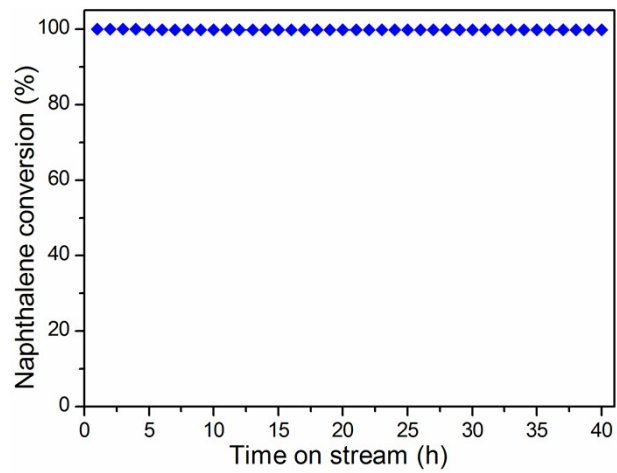
Fig. S11 Long-term stability test with reaction temperature at 270 °C for the 15 wt% Ni_xP-Al-M-(1.25) catalyst.